

1 Production of exotic and conventional quarkonia 2 and open beauty/open charm at ATLAS

3 **C. Bini (on behalf of the ATLAS collaboration.)**

4 Sapienza Università and INFN Roma

5 E-mail: `cesare.bini@roma1.infn.it`

6
7 **Abstract.** The ATLAS experiment at LHC is carrying on a wide programme to
8 study the production properties of conventional and exotic quarkonium, beauty, and
9 charm bound states. The latest results on J/ψ , $\psi(2s)$ and $X(3872)$ production at 7, 8,
10 and 13 TeV, together with D meson production with Run-1 are presented. Studies of
11 associated production of charmonium with vector bosons, searches for exotic states in
12 the bottomonium sector and a new measurement of the ratio of b-quark fragmentation
13 functions are also briefly presented.

14 1. Introduction

15 The production of heavy flavors (HF) in high energy hadron collisions is characterized
16 by a large cross-section. Since the first measurements done at Tevatron [1] it was clear
17 that models based on pQCD were not able to account for such a large production
18 cross-section. The theoretical estimate of these cross-section is a challenge for QCD.
19 Infact many ingredients are needed to obtain consistent estimates to be compared with
20 experimental values, including proton Parton Density Functions (PDFs), hard-scattering
21 cross-sections and hadronization models. Several approaches have been developed
22 in the most recent years to provide theoretical environments for these calculations.
23 Among them the Color Singlet Model (CSM) and the Non-Relativistic QCD (NRQCD
24 including Color Singlet and Color Octet production models) are considered to account
25 for quarkonia production; GM-VFNS (General Mass Variable Flavour Number Scheme),
26 FONLL (Fixed Order + Next to Leading Logs) and MC@NLO and POWHEG
27 complemented by Pythia/Herwig for the hadronization are the methods considered to
28 interpret open HF production. A recent comprehensive review on these models can be
29 found in Ref.[2].

30 In the following we present a summary of the most recent measurements performed
31 by the ATLAS experiment at LHC on quarkonia and open HF production.



32 2. The ATLAS experiment

33 The results presented here are based on the data taken by the ATLAS experiment [3]
34 at LHC during the Run-1 in 2011 and 2012 (7 and 8 TeV c.o.m. energies corresponding
35 to integrated luminosities of ~ 5 and $\sim 21 \text{ fb}^{-1}$ respectively) and on the first data of
36 Run-2 taken in 2015 (13 TeV, $\sim 4 \text{ fb}^{-1}$).

37 The possibility to perform HF physics in ATLAS is based on two main ingredients:
38 low p_T muon triggers and track reconstruction in the inner detector. The muon
39 spectrometer allows to obtain di-muon triggers with muons of p_T down to $4\div 6 \text{ GeV}$ and
40 up to $|\eta| < 2.4$, in an invariant mass region between the J/ψ and the Υ using the RPC
41 (in the barrel) and TGC (in the endcap) trigger detectors. The inner detector provides a
42 tracking in a 2T magnetic field using silicon pixels, silicon strips and transition radiation
43 detectors. In Run-2 an additional pixel layer (the so called Insertable B-layer (IBL))
44 has been added closer to the beam interaction point. Tracks are detected up to $|\eta| < 2.5$.
45 The typical resolution in di-muon invariant mass ranges between 50 MeV (at the J/ψ
46 peak) and 150 MeV (at the Υ peak).

47 In the case of charmonium, two distinct production mechanisms are possible at
48 LHC: prompt and non-prompt production. Prompt particles are directly produced
49 in the primary pp interaction or through feed-down from decays of heavier (directly
50 produced) states; non-prompt particles are produced in the decays of b-hadrons. The
51 two categories can be separated experimentally exploiting the long b-hadron lifetime.
52 The discrimination is based on the so called "pseudo-proper time" τ :

$$53 \quad \tau = \frac{L_{xy} m(\mu\mu)}{|\vec{p}_T(\mu\mu)|} \quad (1)$$

54 where L_{xy} is the travel distance of the quarkonium in the transverse plane, $m(\mu\mu)$ and
55 $\vec{p}_T(\mu\mu)$ are the mass and the transverse momentum of the muon pair respectively.

56 3. Quarkonia production

57 For each considered charmonium final state prompt and non-prompt production cross-
58 sections are obtained separately by counting the events through a combined fit of
59 invariant mass and pseudo-proper time. An example of fit for the $\mu\mu$ final state involving
60 J/ψ and $\psi(2S)$ [4] is shown in Fig.1. All the different contributions are shown. This
61 kind of analysis has been performed for J/ψ [4], $\psi(2S)$ [5, 6], χ_{c1} and χ_{c2} [7]. In general
62 the prompt charmonium production turns out to be well described by NLO NRQCD.
63 Predictions based on NNLO* colour-singlet model calculations clearly underestimate the
64 data, especially at high transverse momenta. The non-prompt charmonium production
65 is reasonably well described by FONLL. The comparison between data and theory for
66 the J/ψ data at 7 TeV c.o.m. energy is shown as a function of $p_T(\mu\mu)$ for different $|\eta|$
67 ranges in Fig.2.

68 The same analysis has been applied on the first bunch of data from Run-2. Fig.3
69 compares the non-prompt fraction as a function of $p_T(\mu\mu)$ of ATLAS data at different

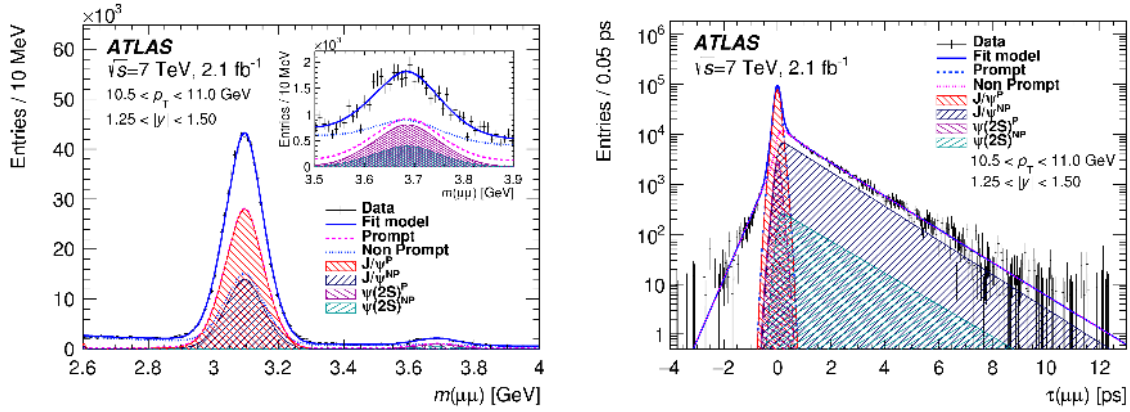


Figure 1. Invariant mass (left plot) and pseudo-proper decay time (right plot) spectra of $\mu\mu$ final states for a given region in $p_T(\mu\mu)$ and $y(\mu\mu)$. The signals of the J/ψ and $\psi(2S)$ (also in the insert of the left plot) can be easily seen. The result of the combined fit is also shown with the detail of the single components.(From Ref.[4])

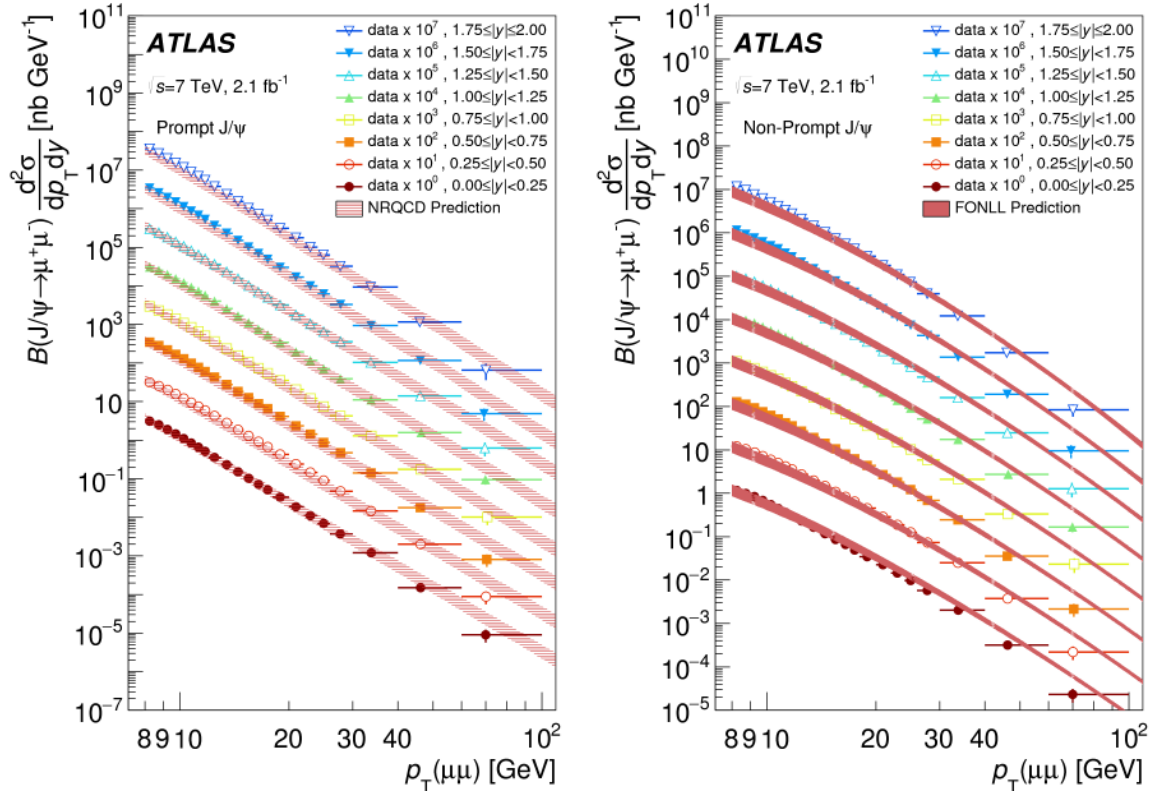


Figure 2. Prompt (left plot) and non-prompt (right plot) J/ψ production cross-section as a function of $p_T(\mu\mu)$ up to 100 GeV in slices of $y(\mu\mu)$. The data are compared with predictions from NRQCD (left) and FONLL (right). A reasonable agreement is found in both cases in a large kinematical range.(From Ref.[4])

70 center of mass energies [8]. The plot includes data from the Tevatron [9] at 1.96 TeV
 71 c.o.m. energy. The comparison shows that the non-prompt fraction behavior with
 72 $p_T(\mu\mu)$ doesn't depend on the c.o.m. energy. Only some discrepancy is observed in the
 absolute scale with respect to lower energy data.

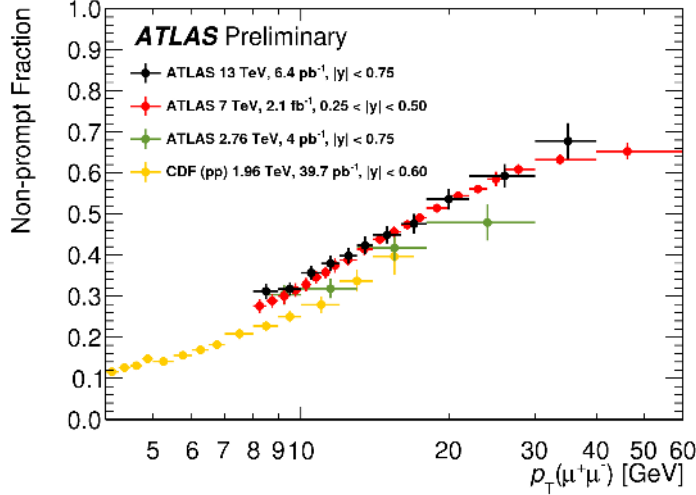


Figure 3. Non-prompt J/ψ production fraction compared to previous measurements from ATLAS in pp collisions at 2.76 and 7 TeV, and from CDF in $p\bar{p}$ collisions at 1.96 TeV. (From Ref.[8])

73

74 In the analysis of the $J/\psi\pi^+\pi^-$ final state [6] we find (see Fig.4), in addition to
 75 the $\psi(2S)$ peak, a clear signal from the X(3872), well-known exotic candidate. A good
 76 description of the prompt X(3872) production cross-section is obtained assuming that
 77 this meson is a mixing of a "molecular state" and a χ_c state [10]. On the other hand
 78 the non-prompt production cross-section is overestimated by all considered models.

79 A search for possible exotic X_b states decaying to $\Upsilon(1S)\pi^+\pi^-$, replica of the X(3872)
 80 in the beauty sector with masses in the range $10.5 \div 10.7$ GeV has been also performed
 81 [11]. No signal is found. Upper limits ranging between 0.02 and 0.03 at the different
 82 masses are obtained for the ratio between X_b and $\Upsilon(2S)$ production.

83 Finally it is worth mentioning the measurement of associated production of the
 84 J/ψ with vector bosons W and Z [12, 13]. In both cases ATLAS finds a cross-section
 85 significantly larger than the one expected by NLO NRQCD calculations. Results with
 86 increased statistical significance are expected soon from Run-2 data.

87 4. Open Charm/Beauty production

88 A systematic study of the production of $D^{*\pm}$, D^\pm and D_s^\pm has been performed [14] using
 89 the final states $K\pi\pi$ and $KK\pi$. D mesons are reconstructed for p_T up to 100 GeV. Fig.5
 90 shows the peaks corresponding to the three mesons in the relevant invariant mass plots.

91

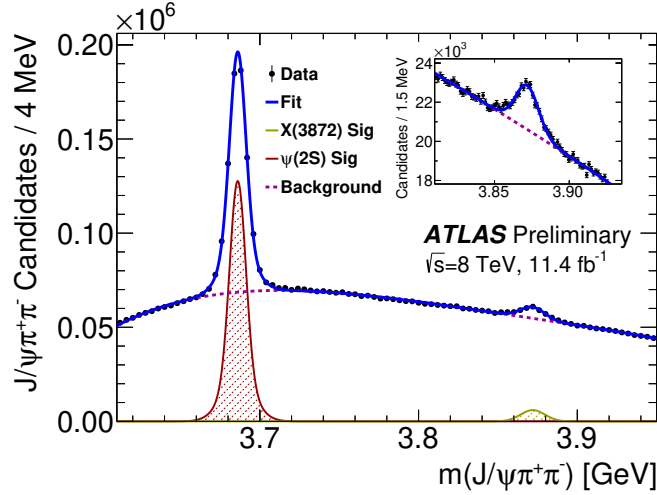


Figure 4. Invariant mass spectrum of $J/\psi\pi^+\pi^-$ with $J/\psi \rightarrow \mu\mu$. In addition to the $\psi(2S)$ peak, a clear signal (see also insert) is observed corresponding to the X(3872) meson.(From Ref.[6])

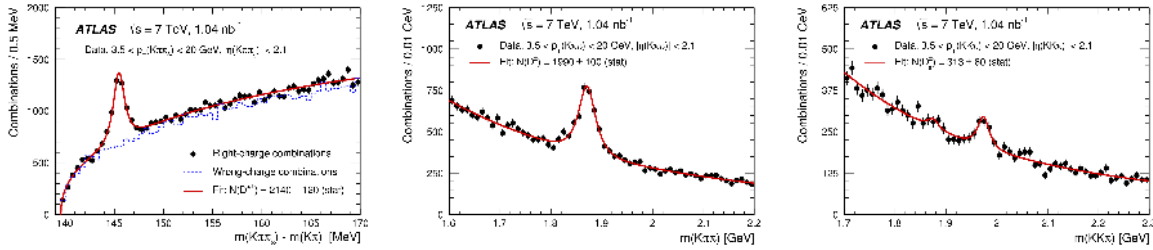


Figure 5. From left to right, three examples of $D^{*\pm}$, D^\pm and D_s^\pm peaks in the p_T and η regions specified in each plot. The number of resulting candidates is also given.(From Ref.[14])

92 The measured D^* and D meson production cross-sections integrated in η are shown
 93 in Fig.6 as a function of $p_T(D)$ and are compared to different models. The best agreement
 94 is obtained in both cases for the GM-VFNS model, that is able to describe both shape
 95 and normalization of the distributions.

96 An important ingredient in the interpretation of the rare B decays is the ratio of
 97 b-quark fragmentation functions f_s/f_d . This quantity can be extracted in pp collisions
 98 from the ratio of the decays $B_d^0 \rightarrow J/\psi K^{*0}$ with $K^{*0} \rightarrow K^+\pi^-$ and $B_s^0 \rightarrow J/\psi\phi$ with
 99 $\phi \rightarrow K^+K^-$. Both decays are observed with high statistics in ATLAS [15] and the
 100 obtained resulting value of f_s/f_d is:

$$101 \quad \frac{f_s}{f_d} = 0.240 \pm 0.004(stat) \pm 0.010(syst) \pm 0.017(th) \quad (2)$$

102 in agreement with results from other experiments. This result extends the knowledge
 103 of this quantity to higher $p_T(B)$ values.

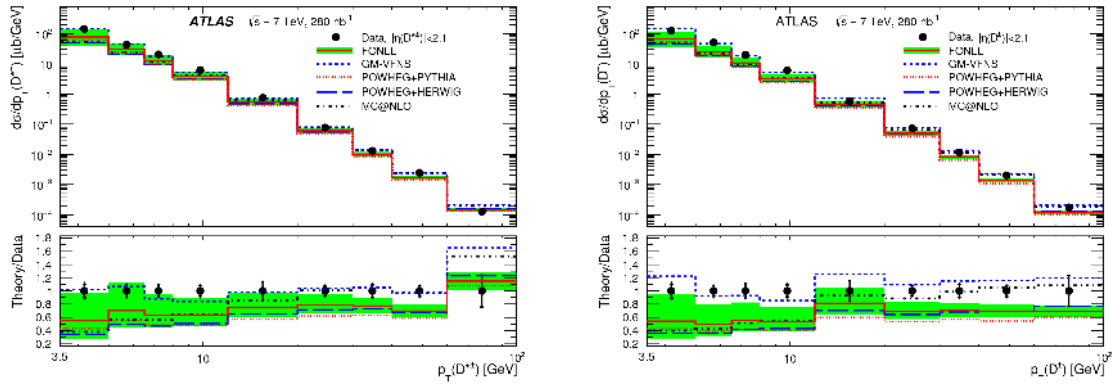


Figure 6. $D^{*\pm}$ (left) and D^\pm production cross-section as a function of $p_T(D)$ and integrated in η . The data are compared with several different predictions. The lower plots show the ratio between theory and experiment.(From Ref.[14])

104 References

- 105 [1] CDF collaboration 1997, *Phys.Rev.Lett.* **79** 572-577
 106 [2] A.Andronic et al. 2015, arXiv:1506.03981v2 [nucl-ex]
 107 [3] ATLAS collaboration 2008, *J. of Instrumentation* **3** S08003
 108 [4] ATLAS collaboration 2016, *Eur.Phys.J. C* **76** 5,283
 109 [5] ATLAS collaboration 2014, *JHEP* **09** 079
 110 [6] ATLAS collaboration 2016, *ATLAS-CONF* **028**
 111 [7] ATLAS collaboration 2014, *JHEP* **07** 154
 112 [8] ATLAS collaboration 2015, *ATLAS-CONF* **030**
 113 [9] CDF collaboration 2005, *Phys.Rev. D* **71** 032001
 114 [10] C. Meng, H. Han and K.-T. Chao 2013, arXiv:1304.6710[hep-ph]
 115 [11] ATLAS collaboration 2015, *Phys.Lett. B* **740** 199-217
 116 [12] ATLAS collaboration 2014, *JHEP* **04** 172
 117 [13] ATLAS collaboration 2015, *Eur.Phys.J. C* **75** 229
 118 [14] ATLAS collaboration 2016, *Nucl.Phys. B* **907** 717
 119 [15] ATLAS collaboration 2015, *Phys.Rev.Lett.* **115** 262001